Anharmonic renormalization of the dispersion of flexural modes in graphene using atomistic calculations

Hengjia Wang and Murray S. Daw
Department of Physics and Astronomy, Clemson University, Clemson, South Carolina 29634-0978, USA
(Received 23 June 2016; revised manuscript received 15 September 2016; published 20 October 2016)

We investigate through an atomistic method the effects of anharmonicity on the dispersion of flexural modes of graphene. Using a calculation based on ensemble averages of correlations among displacements and forces, we calculate the temperature-dependent frequencies for a semiempirical potential for graphene. We find that the dispersion relation of the flexural modes of graphene is renormalized by anharmonic coupling to other modes. Our calculations confirm that the anharmonic continuum results of Mariani and von Oppen [Phys. Rev. Lett. **100**, 076801 (2008)] hold in detail for small wave number and at low temperatures. We examine the deviation from the continuum result outside of that range.

DOI: 10.1103/PhysRevB.94.155434

I. INTRODUCTION

Graphene, like any membrane, is expected to have long-wavelength, out-of-plane (so-called "flexural") modes. If the membrane is stress-free, the dispersion of those modes should be quadratic in wave number (that is, $\omega \propto k^2$) when the harmonic approximation holds [1–3]. Anharmonicity may modify the dispersion relation, which would affect the transport of heat in the material. Some authors suggest that the flexural modes may in fact dominate the lattice thermal conductivity of graphene [4,5]. Anharmonic coupling of the flexural modes to in-plane modes have been shown to stabilize the sheet with respect to rippling [6–8]. The coupling of the flexural modes to electrons also has significant effect on the electrical conductivity [9].

The effect of anharmonicity on the dispersion relation of the long-wavelength flexural modes was considered in the continuum limit by Mariani and von Oppen [10]. Following Nelson and Peliti [6], they began with the potential energy of nearly flat graphene, including corrections to the harmonic potential that are lowest order in wave vector and amplitude, which then couple the flexural modes to in-plane modes. Assuming classical dynamics, the in-plane modes were integrated out, leaving an effective, temperature-dependent interaction among the flexural modes. They then applied a one-loop renormalization group analysis to this effective Hamiltonian to demonstrate that the coupling of flexural modes to the in-plane modes renormalizes the dispersion of the flexural modes. They found that the frequency ω of a flexural mode with wave vector k at temperature T is given by [11]

$$\omega = \alpha(T,k)k^2, \tag{1}$$

in which

$$\alpha(T,k) = \alpha_0\left[1 + \frac{k_c^2}{k^2}\right]^{1/4}, \tag{2}$$

where the temperature dependence is carried by wave vector scale k_c, which varies as $T^{1/2}$. These results show that $\omega \sim k^2$ at low temperatures as expected, while $\omega \sim k^{3/2}$ at high temperature. Their analysis is expected to hold for low k and T, but they do not determine the range of k and T for which the analysis is expected to hold.

As has been observed experimentally [12–14] and analyzed theoretically [8], free-standing graphene sheets are unstable to rippling of characteristic length on the order of 50–200 Å at room temperature. Atomistic simulations using bond order potentials [15] have confirmed rippling when the simulation cell sizes were sufficiently large; for cells smaller than the Ginzburg length [6] the ripples are suppressed and the sheet remained relatively flat. The analysis of MvO is based on perturbation around flat graphene.

We apply here an atomistic method [16–19] (which we call the "moments method"), implemented here for interatomic potentials, for calculating the temperature-dependent frequency. Our simulations are performed on cells smaller than the Ginzburg length which would inhibit rippling, and therefore should be compared directly to the results of MvO. Our results confirm that the dispersion relations are renormalized and that the form of Mariani–von Oppen holds in the region of low k and T. We also note deviation from their form outside of that region, determining then the range of validity of their approach.

We begin by a brief recap of the moments method, and then show our results for the renormalized dispersion relation, ending with a discussion and summation.

II. METHOD

The moments method is an approximation based on low-order moments of the Liouvillian operator [16], which is the time-evolution operator for a classical dynamical system. Beginning with the harmonic force constant matrix, the normal modes are found, indexed by wave vector k and branch b. (The flexural modes are easily identified by their low frequency and out-of-plane polarization.) Using the harmonic modes as a basis is justified by the weakly anharmonic character of this system. The second moment of the power spectrum of the displacement-displacement autocorrelation (suppressing in the rest of this paper the branch index for simpler presentation)

$$\mu_2(k) = \frac{\langle \dot{A}_k^2 \rangle}{\langle A_k^2 \rangle} = -\frac{\langle A_k \ddot{A}_k \rangle}{\langle A_k^2 \rangle} \tag{3}$$

(where the angle brackets indicate ensemble averages) give a simple measure of the quasiharmonic, temperature-dependent

normal mode frequencies $\omega(k)$

$$\omega(k) = \sqrt{\mu_2(k)}. \tag{4}$$

All of the results we report here are for classical dynamics, with canonical ensemble averages, as was assumed in the approach of Mariani and von Oppen (following Nelson and Peliti).

The classical ensemble averages are evaluated using standard Monte Carlo techniques. The amplitude A_{kb} of each mode is determined by projection onto the harmonic normal modes. The energy differences for the Metropolis algorithm, as well as the accelerations in each mode, are obtained in the present work by semiempirical interatomic interactions. We have done calculations with the original Tersoff potential for carbon [20], and also with the modified Tersoff potential which is tailored for graphene [21]. We will show here the results for the modified Tersoff potential. The results for the original Tersoff potential are qualitatively very similar, though there is some quantitative difference, and we will note the differences where they exist. Using a semiempirical potential such as the Tersoff potential effects a compromise between speed and accuracy, though the anharmonic effects are reasonably well captured by especially the modified potential [21].

The computational cell is a 1152-atom graphene sheet about 60 Å along one edge with triclinic periodic boundary conditions consistent with the sixfold rotational symmetry of graphene. The Monte Carlo calculation included 4.6×10^7 steps. The periodic boundary conditions limit the modes included in the calculation to those whose wave vectors are commensurate with the supercell, and also inhibits rippling. The lattice parameter of the cells is determined at each temperature by molecular dynamics with adjustable cell size at constant (zero) pressure, thus incorporating thermal expansion or contraction. The statistical quality of the sampling is tested and discussed in the following text. All of the modes present in the cell are included in the calculation, but we focus here only on the flexural modes.

III. RESULTS

Figure 1 shows the dispersion relation of the flexural modes calculated by this method at two different temperatures. The points are the atomistic results and the curves are simple power law fits to the points [22]. The results shown here at $T = 0$ K are actually from the harmonic force constants determined from the current cell, but they differ negligibly from what we obtain by the moments method at very low temperature. At $T = 0$ K, the best power-law fit is to a quadratic dispersion. The value of α_0 is determined to be 62.8 Å^2 THz by this quadratic fit, compared with the value of 62 Å^2 THz obtained via first-principles calculations by Mingo and Broido [1,23]. At the higher temperature ($T = 1200$ K) the best power-law fit is to $k^{1.8}$ (for the original Tersoff, $k^{1.7}$), which is inside of the range of behavior of the continuum calculations. We have calculated the dispersion at several other temperatures between 0 and 1200 K, and the dispersion curves fall in between those of the two extreme temperatures.

As is obvious from Fig. 1, the change in dispersion relation with temperature is subtle. To make a precise comparison between the atomistic and continuum results, we note that

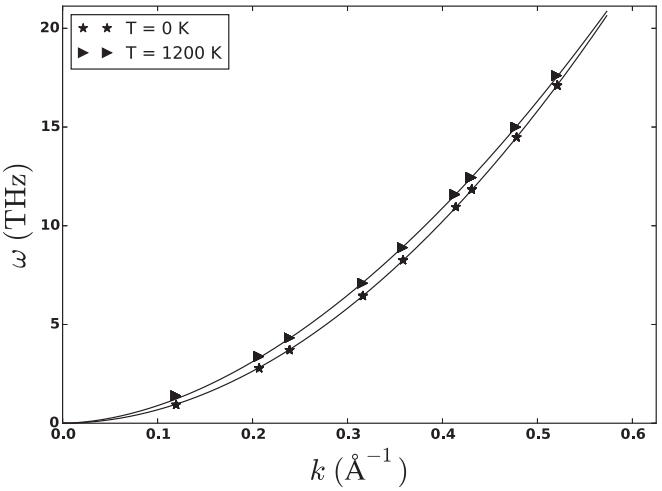

FIG. 1. Dispersion of the flexural modes, calculated using the moments method at two temperatures ($T = 0$ K and 1200 K). The points are the results of our calculations, and the lines are simple power-law fits. These results are for the modified Tersoff potential. The dispersion curves for several intermediate temperatures have been calculated and are smooth intermediates to these curves, so they have been omitted from this plot for the sake of presentation.

Eqs. (1) and (2) establish a peculiar relation between ω, k, and T. In particular, a little rearrangement gives

$$\frac{\omega^4}{k^6} = \alpha_0^4\left(k_c^2 + k^2\right), \tag{5}$$

where all of the wave vector dependence on the right-hand side is in the k^2 term and all of the temperature dependence enters into $k_c^2 = \beta T$, where β is a constant. Plotting (ω^4/k^6) vs k^2 should then reveal a series of parallel straight lines at low temperatures, shifted by temperature. The vertical intercepts are a measure of the anharmonicity and should scale linearly with temperature.

This replotting of the calculated, temperature-dependent dispersion curves is done according to Eq. (5) in Fig. 2, where now we include all of our calculated temperatures. The points are atomistic results and the solid lines simple linear fits to the points, such that the slope of each is fixed by the harmonic ($T = 0$ K) calculations. This leaves one parameter used for the fit at each temperature above $T = 0$ K, which is the vertical offset. In this plot, we do the fit only for modes with k below 0.4 Å^{-1}, above which there is some deviation.

By subtracting off the k-dependent part of Eq. (5) we can isolate the temperature dependence:

$$\frac{\omega^4 - \omega_0^4}{k^6} = \alpha_0 \beta T, \tag{6}$$

where ω_0 is the frequency of the mode at $T = 0$ K. We again replot the calculated results for T below 200 K according to this form in Fig. 3, where the lines are simple horizontal fits (for the first five k vectors), and they illustrate in a clearer way the quality of the fits in Fig. 2 at low temperatures.

(A word about the error bars in Figs. 2 and 3 is in order. The rotational symmetry of graphene determines that there are sets of symmetry-equivalent k vectors. Because our Monte Carlo sampling does not enforce the rotational symmetry of the

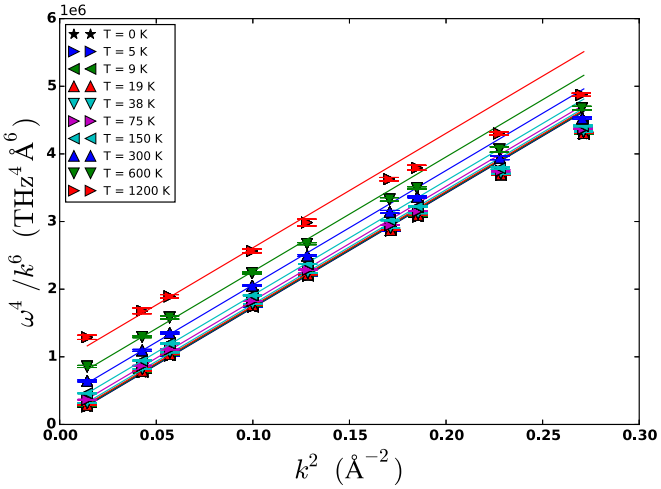

FIG. 2. Plot of (ω^4/k^6) vs k^2 at various temperatures. Points are the results of the present calculation. The lines are simple, one-parameter fits to the values for the lowest five k vectors. The single parameter for each temperature is the vertical offset, the slope for all being determined by the $T = 0$ K calculations. Error bars are statistical, as discussed in the text.

graphene, the variation we find among each set is a measure of the statistical quality of the sampling in this calculation. The calculated results plotted in these figures are determined by examining the statistical variation among those symmetry-equivalent k vectors: the points are the averages, and the error bars are the rms deviation.)

The intercepts in Fig. 2 give the values of k_c^2. We then plot k_c^2 vs temperature in Fig. 4 to test the prediction that k_c^2 should be linear in T. The points are atomistic results and the line is a linear fit to the low-temperature calculations below 200 K, showing that the relation $k_c^2 \propto T$ is followed at low

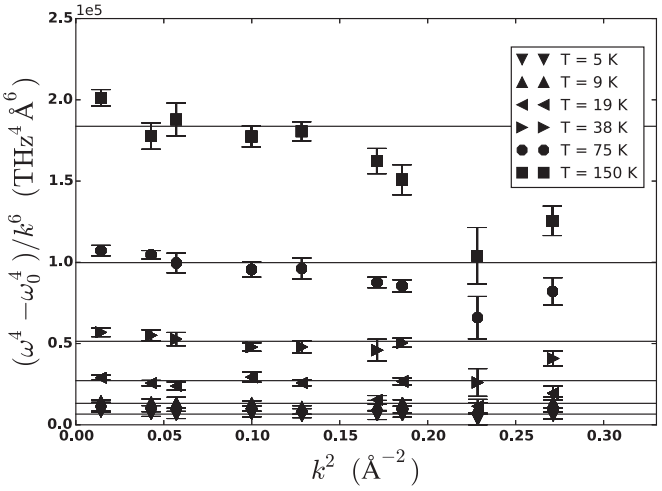

FIG. 3. Plot of $(\omega^4 - \omega_0^4)/k^6$ vs k^2 at low temperatures. This is a replotting of the calculations from Fig. 2 to emphasize the temperature dependence. Points are the results of the present calculations, and the horizontal lines are simple fits to the values of the lowest five k vectors. Error bars are statistical, as discussed in the text.

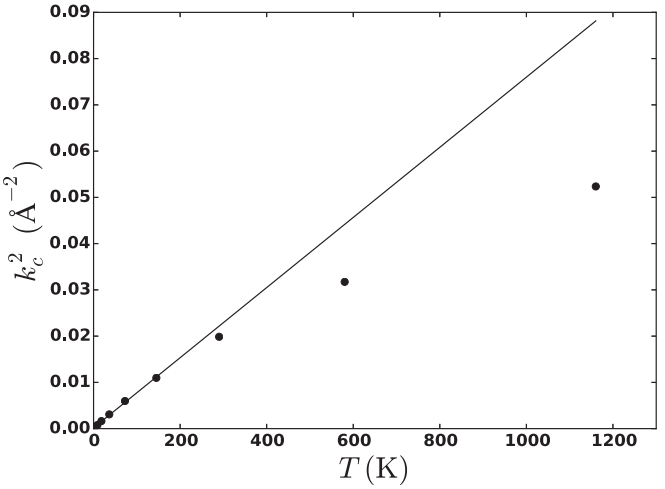

FIG. 4. Plot of k_c^2 vs T, showing the linear behavior at low temperatures predicted by Mariani and von Oppen [10]. The points are our calculations, and the line is a one-parameter linear fit to the lower temperature calculations.

temperatures, where the approach of Mariani and von Oppen is expected to have the best success.

In Fig. 5, we replot the calculations from Fig. 4, now in log-log form, to demonstrate that the slope in Fig. 5 for temperatures below $T = 200$ K is close to 1, confirming that k_c^2 is linear in T at low T but deviates at higher T.

Finally, considering our results altogether, we are able to get a good fit to all of our calculated points up to $k = 0.4$ Å^{-1} and $T = 200$ K to the form of Mariani and von Oppen using just two parameters (α_0 and β). The value of β determined overall is 2.0×10^{-4} Å^{-2}K^{-1}, which is a little higher than the value calculated from MvO (6.1×10^{-5} Å^{-2}K^{-1}). For larger values of k or higher T, there is some deviation as noted.

The results shown here are for the modified Tersoff potential. We have also performed the same calculations using the original Tersoff potential, and find that the agreement with

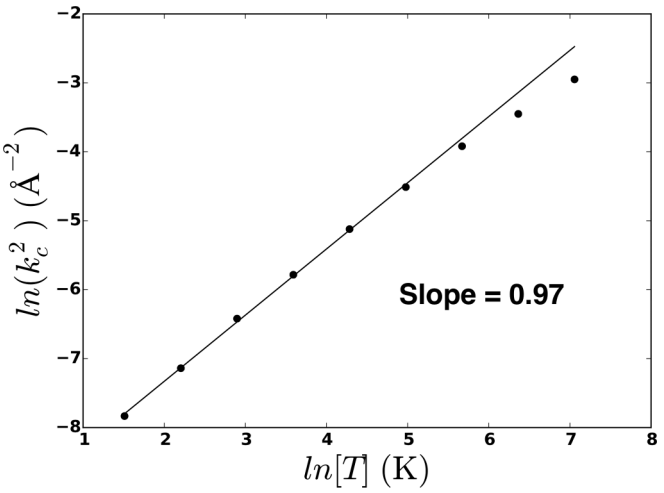

FIG. 5. Plot of $\ln(k_c^2)$ vs $\ln(T)$, along with a linear fit to the lower temperature calculations. The continuum theory predicts a slope of 1 [10].

the form predicted by Mariani and von Oppen is the same for low T and k, and that the deviation outside of that range is similar. The original Tersoff matches the continuum results over a larger range of k, agreeing out to $k = 0.5$ Å^{-1}. The value of β is smaller for the original Tersoff than the modified Tersoff by an order of magnitude (3.3×10^{-5} Å^{-2}K^{-1}). This difference in β is consistent with the stronger anharmonicity of the original Tersoff. (The modified Tersoff potential was the result of an attempt to tone down the anharmonicity, to bring the calculated value of lattice thermal conductivity closer to experiment [21].)

IV. CONCLUSIONS

We have presented results obtained for the temperature-dependent dispersion relation of flexural modes in graphene. These results have been obtained using a method based on Monte Carlo averages of displacements and forces. In the present calculation the energies and forces required for the MC calculation were obtained using two versions of the semiempirical Tersoff potential—the original version for diamond and another modified for graphene.

We then analyzed the dispersion relation to show that our results confirm the nonlinear continuum results of Mariani and von Oppen. Mariani and von Oppen's approach is based on a perturbative expansion of the potential energy and is therefore expected to be good at low T and k. Our results (based on a semiempirical potential) represent a more robust potential energy surface, and should hold out to higher k and T. It is encouraging to see that the two very different approaches (continuum vs atomistic) yield the same behavior in the low k and low T region. Furthermore, the continuum calculations did not establish the range of temperatures or wave vectors for which the expansion is expected to hold. Our calculation shows that their approximation works well up to temperature and wave vector noted, and that even outside of that range the form is not an unreasonable approximation to our results. The agreement also serves as a test of the atomistic method, showing that it is able to handle a rather subtle anharmonic feature of the vibrational modes.

ACKNOWLEDGMENTS

We thank Dr. Ted Dickel (Mississippi State University) for helpful suggestions during this work. Our research was supported by the US Department of Energy, Office of Basic Energy Science, Division of Materials Sciences and Engineering under Grant No. DE-SC0008487.

[1] N. Mingo and D. A. Broido, Phys. Rev. Lett. **95**, 096105 (2005).
[2] L. Landau and E. Lifshitz, *Theory of Elasticity* (Pergamon, New York, 1986).
[3] M. Mohr, J. Maultzsch, E. Dobardzic, S. Reich, I. Milosevic, M. Damnjamovic, A. Bosak, M. Krisch and C. Thomsen, Phys. Rev. B **76**, 035439 (2007).
[4] L. Lindsay, D. A. Broido, and N. Mingo, Phys. Rev. B **82**, 115427 (2010).
[5] D. L. Nika, E. P. Pokatilov, A. S. Askerov, and A. A. Balandin, Phys. Rev. B **79**, 155413 (2009).
[6] D. Nelson and L. Peliti, J. Phys. (Paris) **48**, 1085 (1987).
[7] D. Nelson, T. Piran, and S. Weinberg, *Statistical Mechanics of Membranes and Surfaces* (World Scientific, Singapore, 2004).
[8] I. V. Gornyi, V. Yu. Kachorovskii, and A. D. Mirlin, Phys. Rev. B **92**, 155428 (2015).
[9] I. V. Gornyi, V. Yu. Kachorovskii, and A. D. Mirlin, Phys. Rev. B **86**, 165413 (2012).
[10] E. Mariani and F. von Oppen, Phys. Rev. Lett. **100**, 076801 (2008); **100**, 249901(E) (2008).
[11] Note that the sixfold rotational symmetry of graphene insures that the dispersion relation for small k will be isotropic (that is, independent of the direction of k). Further out in the Brillouin zone, the dispersion relation depends as well on direction of k.
[12] J. C. Meyer, A. K. Geim, M. I. Katsnelson, K. S. Novoselov, T. J. Booth, and S. Roth, Nature (London) **446**, 60 (2007).
[13] D. A. Kirilenko, A. T. Dideykin, and G. Van Tendeloo, Phys. Rev. B **84**, 235417 (2011).
[14] P. Xu, M. Neek-Amal, S. D. Barber, J. K. Schoelz, M. L. Ackerman, P. M. Thibado, A. Sadeghi, and F. M. Peeters, Nat. Commun. **5**, 3720 (2014).
[15] A. Fasolino, J. H. Los, and M. I. Katnelson, Nat. Mater. **6**, 858 (2007).
[16] Y. Gao, D. Dickel, D. Harrison, and M. Daw, Comput. Mater. Sci. **89**, 12 (2014).
[17] Y. Gao and M. Daw, Model. Simul. Mater. Sci. Eng. **23**, 045002 (2015).
[18] Based on the moments formalism [17], a package called *Jazz* was implemented to calculate lifetimes and frequencies of normal modes in anharmonic systems. *Jazz* is a python wrapper for LAMMPS [19] (http://lammps.sandia.gov) and does Monte Carlo averages to give lifetimes and frequencies mode by mode. Generally the package works with any potential available in LAMMPS, and the public version is freely available on the SourceForge website (https://sourceforge.net/projects/jazzforlammps).
[19] S. Plimpton, J. Comput. Phys. **117**, 1 (1995).
[20] J. Tersoff, Phys. Rev. B **39**, 5566 (1989); **41**, 3248 (1990).
[21] L. Lindsay and D. A. Broido, Phys. Rev. B **81**, 205441 (2010).
[22] As noted earlier [11], near the Brillouin zone center the dispersion for graphene is isotropic (depends only on the magnitude of k). The k vectors used in Fig. 1 have various directions, but—as the figure shows implicitly—they are close enough to the center that the dependence of the frequency on direction is very weak, so we are able to plot the dependence that way.
[23] Our value of α_0 determined this way for the original Tersoff is 44.9 Å^2 THz.